Journal of Ovonic Research Vol. 6, No. 1, February 2010, p. 63-74

# ELECTRICAL AND OPTICAL PROPERTIES OF SOL-GEL PREPARED Pd-DOPED $SnO_2$ THIN FILMS: EFFECT OF MULTIPLE LAYERS AND ITS USE AS ROOM TEMPERATURE METHANE GAS SENSOR

SANDIPAN RAY[b*], P. S. GUPTA[a], GURDEEP SINGH[b]
[a]*Department of Applied Physics, I.S.M.U., Dhanbad, Jharkhand, India*
[b]*Department of Environmental Science and Engineering, I.S.M.U., Dhanbad, Jharkhand, India*

Tin dioxide thin films of multiple layers were prepared from a chloride-based inorganic salt by sol-gel method. The multilayered films were subjected to optical and XRD studies. The carrier concentrations of the films were calculated and studied. A comparative analysis of different multilayered films of both undoped and Pd-doped $SnO_2$ thin films have been carried out in the presence of methane gas to investigate the possibility of its use as room temperature sensor for methane gas.

(Received Februarie 27, 2010; accepted March 15, 2010)

*Keywords:* $SnO_2$ thin films; XRD; Absorption spectra; Methane sensing

## 1. Introduction

Explosion due to methane gas leakage is one of the most potential hazard in the underground coalmines. Mixture of methane with air is explosive within the range 5-14% by volume of methane. To prevent this hazard, different types of methane detectors have been developed in the market, each with certain advantages and disadvantages. The basic differences lie in their sensing technologies.

Detection of hazardous gases has always been a complex subject and makes choosing an appropriate gas-sensing metal oxide a difficult task. Different gas sensitive metal oxides have been identified and used in the field of air quality monitoring and industrial safety[1,2,3]. But till date no such gas sensors exist that are hundred percent selective to a single gas. Achieving such selectivity requires the use of instruments that employ analytical techniques to identify gases. The use of $SnO_2$ as gas sensors and study of the sensing properties such as the sensitivity and selectivity using dopants are under way to meet their ever-expanding demands in new applications[4,5,6,7].

Tin(IV) oxide is a semiconductor with a direct forbidden band gap of 3.6 eV and it is amenable to n-type doping. The carrier electron gas becomes degenerate at doping levels above about $5 \times 10^{18}$ $cm^{-3}$. Adsorption of oxygen on the oxide surface leads to the trapping of carriers by acceptor states localized on oxygen. However, reaction between the adsorbed oxygen and reducing species such as CO, $CH_4$ or $C_2H_5OH$ in a catalytic oxidation process releases carriers back into the solid. The associated changes in resistance form the basis for the application of tin oxide as a sensor for the detection of reducing gases.

The present work reports a comparative study of various optical and electrical properties of different multilayer undoped and palladium doped $SnO_2$ thin films in presence of methane. Most of the works with $SnO_2$ based methane gas sensors are reported for high temperatures as it is quite difficult to get a good response for methane at low temperatures. A humble effort was made in this study to observe the changes in gas sensitivity at room temperature against the increase in

*Corresponding author: write_2_sandipan@yahoo.co.in

film thickness. With further palladium doping the $SnO_2$ multilayered thin films showed an interesting phenomenon in presence of methane gas.

## 2. Experimental details

Reagent grade(Merk) $SnCl_2.2H_2O$ was used as precursor material. 8.374 gm of $SnCl_2.2H_2O$ was dissolved in 100 ml of absolute ethanol. The mixture was refluxed and stirred at 353 K for 3 hours and then it was allowed to cool to the room temperature for 1½ hours with continuous stirring. A commercial spin coater (Apex SCU 2005) was used for coating the sol on the glass substrates. The speed of the spin coater was fixed at 2100 rpm. Six drops (0.8 ml = 6 drops) of sol were dropped on approximately 1 inch x 1 inch sized clean glass slide. The coated glass slide was air annealed at 673 K for 10 minutes. The slide was then allowed to cool to the room temperature to produce a transparent $SnO_2$ film. Using the above procedure multilayered films (starting from 1-layer to 12-layers) were prepared. Every layer was deposited repeating the same procedure and conditions as before.

These multilayered films were then characterized with XRD and their optical studies were done using UV-Vis-NIR Spectroscope to calculate the band gap of the films.

To increase the sensitivity, the multilayered films were doped with palladium. 0.05% solution of palladium chloride was made with ethanol. It was stirred for 1 hour at 50$^o$C and was then allowed to cool to the room temperature while stirring. The prepared sol was then spin coated over $SnO_2$ to obtain the doped tin dioxide multilayer samples. The spin coating speed, number of drops applied, the annealing temperature and time are all kept same as those for the undoped samples.

Small pieces of dimension 0.5 x 0.5 sq. cm of the films were used for sensitivity measurements of both undoped and doped multilayered films. Methane gas diluted with argon gas in a definite concentration of 1500 ppm was introduced into the gas chamber. A digital multimeter (Agilent 34401A) and a constant voltage source (Caddo Programmable DC Power Supply) were used to calculate the change in the resistances of the multilayered films in the range 0 to 28 V. The measurements were carried out initially in vaccum and then in the presence of methane gas at room temperature both for undoped and Pd-doped $SnO_2$ films.

### 2.1 Experimental setup

The gas sensing chamber (fig 1) used for gas sensitivity analysis of the prepared films consist of a steel base with three port holes at the base for insertion of more than one gas at the same time. This helps us to generate the exact mining ambient conditions inside the chamber. Above the steel base there is a raised sample holder made of copper which is placed over a heating coil to raising the temperature of the film. The film placed above the sample holder is connected by two probes which are further connected in series with a Programmable D.C. Power Supply and a Digital Multimeter. The thermocouple as shown in the diagram keeps track of the rise in temperature of the sensing material (though not required in the present study as it was done at room temperature). The whole system is covered by a glass chamber fitted with rubber tube at its base to ensure complete vacuum in the chamber through suction by a high capacity vacuum pump. The chamber is well developed for controlled variations of the inner atmospheric temperature and pressure for controlled gas sensing analysis.

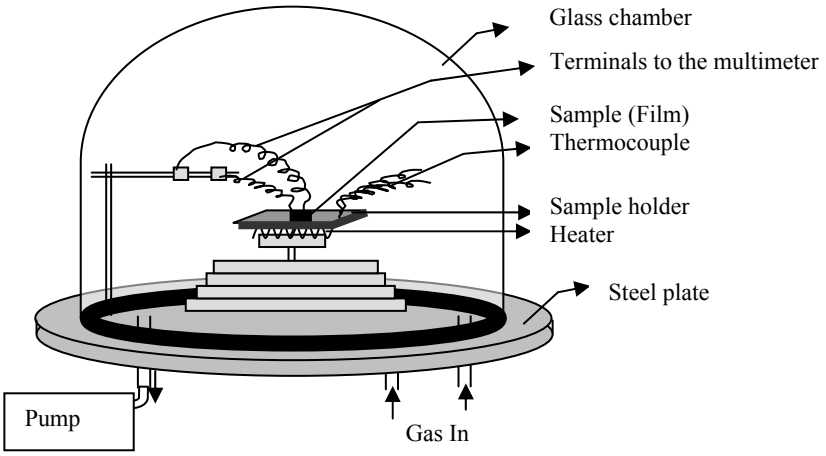


*Fig.1. Schematic diagram of the gas sensing unit used for sensor characteristics measurements.*

## 3. Results and discussion

### 3.1. XRD studies

X-ray diffraction pattern for the deposited $SnO_2$ thin films for single layer and multilayers were obtained. All the samples were prepared under identical conditions. Thin $SnO_2$ films starting from single layer to twelve layers were deposited and characterized with similar conditions and results of some are shown in fig.2&3.

The deposited films upto three layered undoped $SnO_2$ showed amorphous nature whereas with increase in the number of layers, crystalline nature of the deposited $SnO_2$ films sets in. Reflections from the tetragonal crystallographic phase (cassiterite) of $SnO_2$ became more defined and progressively more intense and sharp for films with more than five layered depositions. The XRD spectra of the deposited undoped $SnO_2$ films (fig2) show reflection from the (110), (101), (200), (211) and (310) planes of $SnO_2$ for 2θ values of $26.8^o$, $34.05^o$, $38.12^o$, $51.9^o$ and $65.51^o$, respectively. These results comply with the standard $SnO_2$ XRD pattern of the JCPDS lines[8] as shown in the fig. 4.

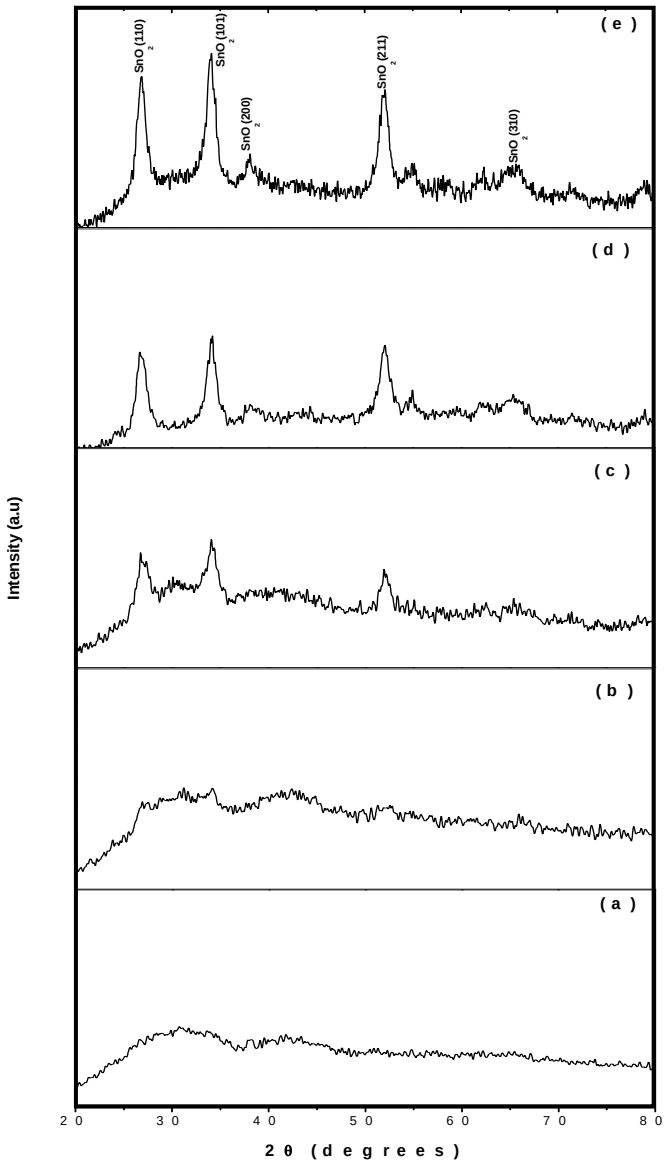


*Fig.2. X-ray diffraction patterns of the undoped $SnO_2$ thin films with varying deposition layers. (a)1-layered (b) 3-layered (c) 6-layered (d) 8-layered (e) 12-layered*

Similar XRD pattern, shown in fig 3, have been obtained for Pd-doped coatings over $SnO_2$ thin films. The Pd-doped upto three layered $SnO_2$ films showed amorphous nature. For all the other Pd-doped $SnO_2$ XRD spectras, addition of Pd peaks and slight reduction in intensity of the $SnO_2$ peaks are observed. The XRD spectra for Pd-doped $SnO_2$ shows reflections from the (110) and (220) planes of palladium for 2θ values of $40.65^o$, and $72.56^o$ respectively. The predominant peaks for eight layered (fig 2(d)&3(d)) and twelve layered (fig 2(e)&3(e)) $SnO_2$ films can be explained as the cumulative effect of the annealing temperature and time during every single layer deposition. This shows increase in mean grain size and improved crystallinity.

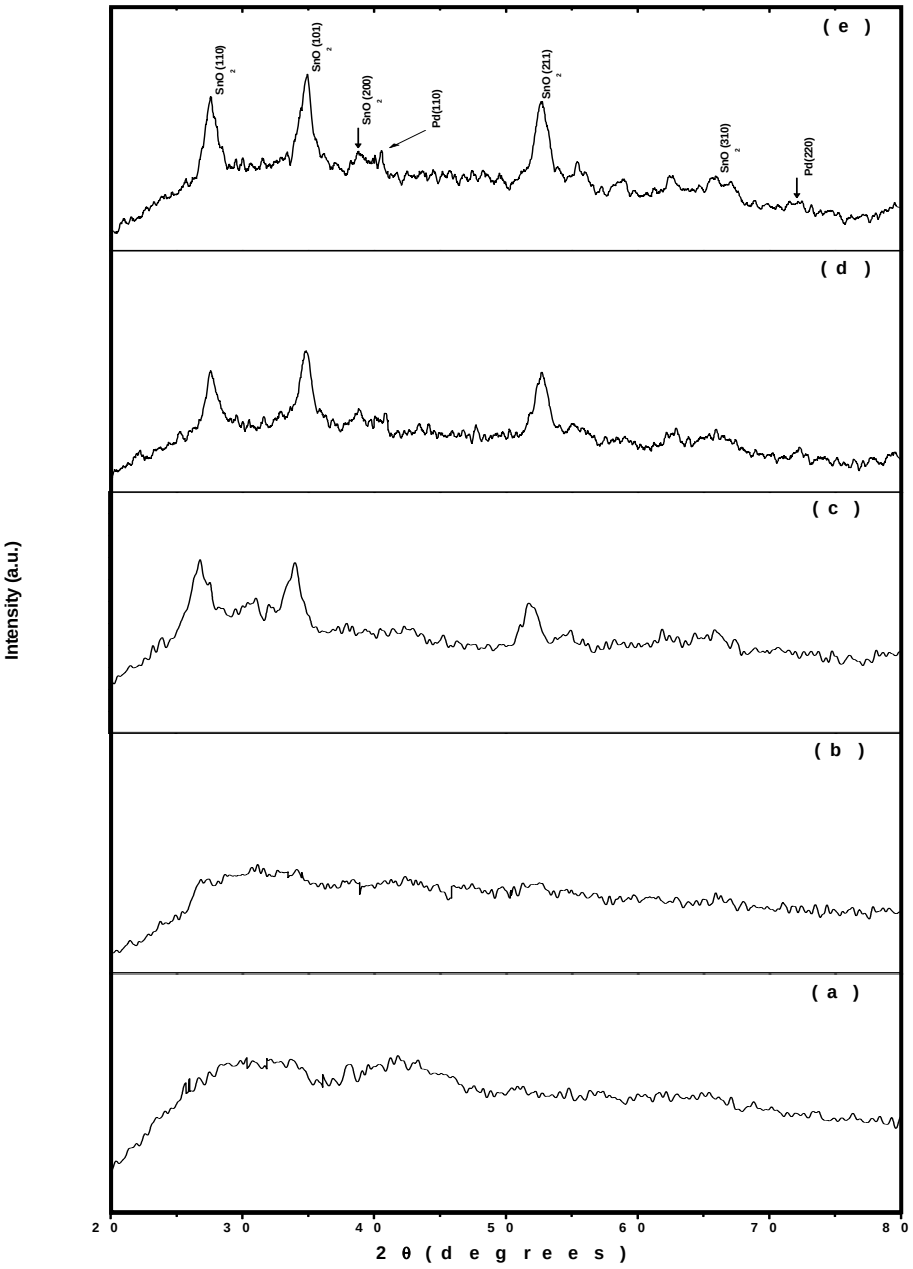


*Fig.3: X-ray diffraction patterns of the Pd-doped $SnO_2$ thin films with varying deposition layers. (a)1-layered (b) 3-layered (c) 6-layered (d) 8-layered (e) 12-layered*

For calculating the particle size of the deposited films, the Debye-Scherrer formula was employed on the XRD spectras of the twelve layered and the eight layered $SnO_2$ films which is given as $d = (0.9\lambda / \beta \cos \theta)$ where, $\lambda$ is the wavelength of the X-ray employed which in this case is 0.15418 nm for Cu-$k_\alpha$. $\beta$ is the FWHM (full-width at half maxima) and $\theta$ is the Bragg's angle in degrees. Calculating 'd' from the best two XRD patterns, it has been found that the average particle thickness of the prepared eight layered and twelve layered Pd-doped films is about 28.3 nm and 31.2 nm respectively.

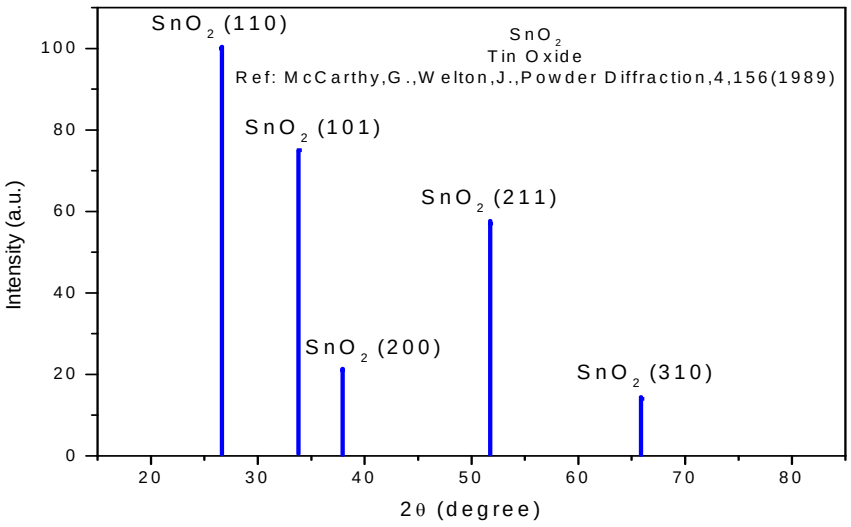


Fig. 4. JCPDS reference lines for $SnO_2$.

### 3.2. SEM studies

Surface morphologies obtained through Scanning Electron Microscope (SEM) of undoped and Pd-doped $SnO_2$ films are shown in fig. 5. Fig. 5(a) shows a comparatively smoother film surface for three layered undoped $SnO_2$ which is amorphous in nature as observed from the XRD spectra. For six layered undoped $SnO_2$ (fig.5(b)), the film surface does not look much different from that of fig 5(a). However with further increase in the number of film layers i.e. for twelve layered $SnO_2$ (fig 5(c)), we find considerable roughness on the film surface showing increase in grain growth. This can be correlated with the predominant XRD peaks as obtained for the twelve layered $SnO_2$ (fig. 2(e)). SEM images for palladium doped films (fig 5(d),(e)&(f)) show better surface roughness with increased grain growth.

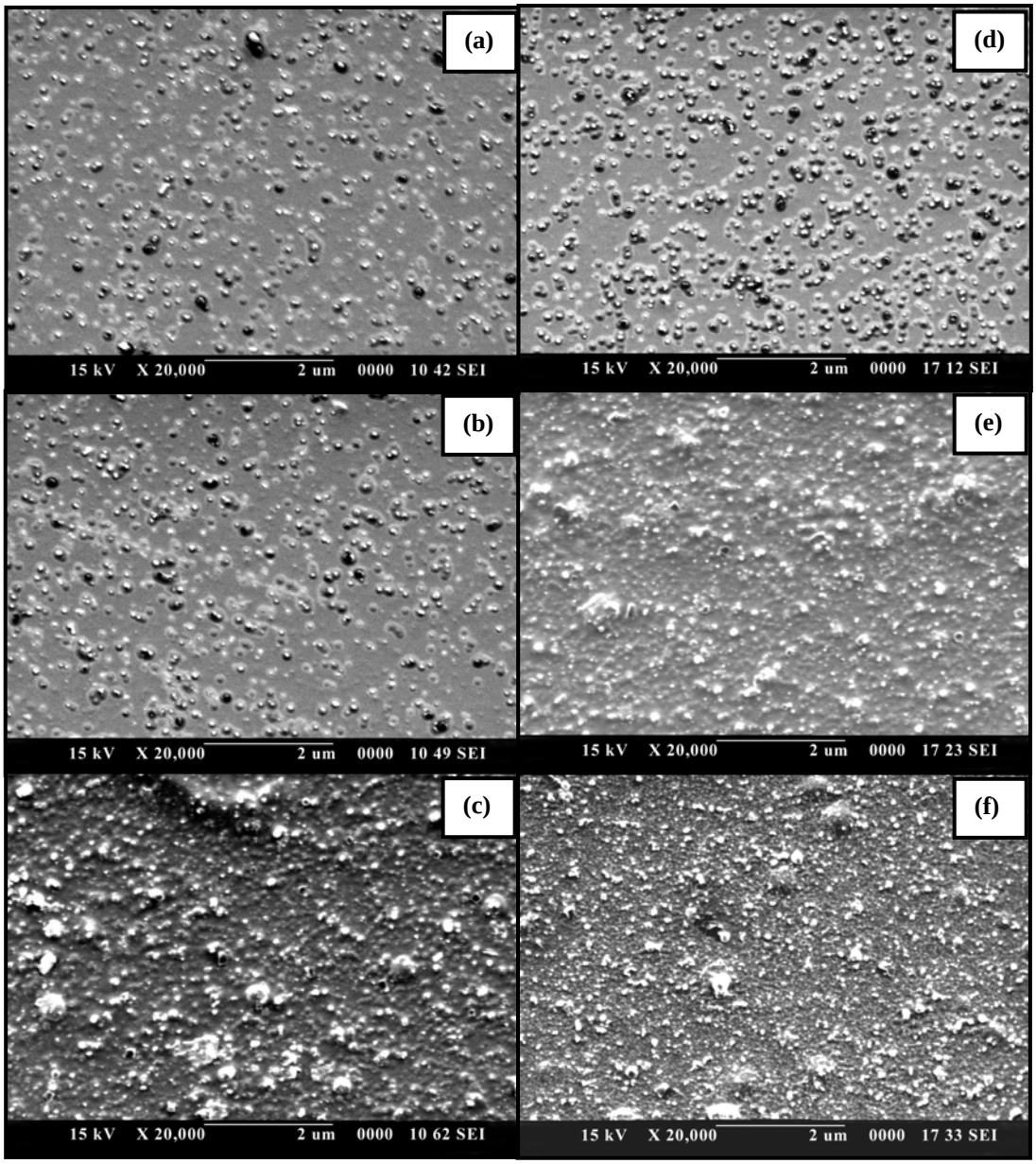


*Fig.5. SEM images of $SnO_2$ thin films with varying deposition layers. (a) 3-layered undoped $SnO_2$ (b) 6-layered undoped $SnO_2$ (c) 12-layered undoped $SnO_2$ (d) 3-layered Pd-doped $SnO_2$ (e) 6-layered Pd-doped $SnO_2$ (f) 12-layered Pd-doped $SnO_2$*

### 3.3. Optical studies

The optical studies of the films were carried out using UV-Vis-NIR Spectroscope and the spectral dependence of the transmittance (T) for one, three, six, eight, ten and twelve layered films are shown in fig.6(a) & (b) and fig.7(a) & (b). The average transmission of the undoped $SnO_2$ films deposited on glass substrates is more than 80% over the range 450 to 800 nm. A sharp fall in transmission at about 310 nm is due to the absorption of the glass substrate. The transparency of the films decreases in major portions of the visible range with the addition of layers. This may be due to the built-up thickness which is also clear from the fringes in the transmission spectra. The absorption edge also shifted slightly to higher wavelengths with the increase in film layers. The transmittance falls rapidly in the low wavelength region. With increase in number of layers, the

onset of absorption edge becomes less sharp, this may be due to the presence of bigger crystalline sizes and increased scattering due to the surface roughness [9,10].

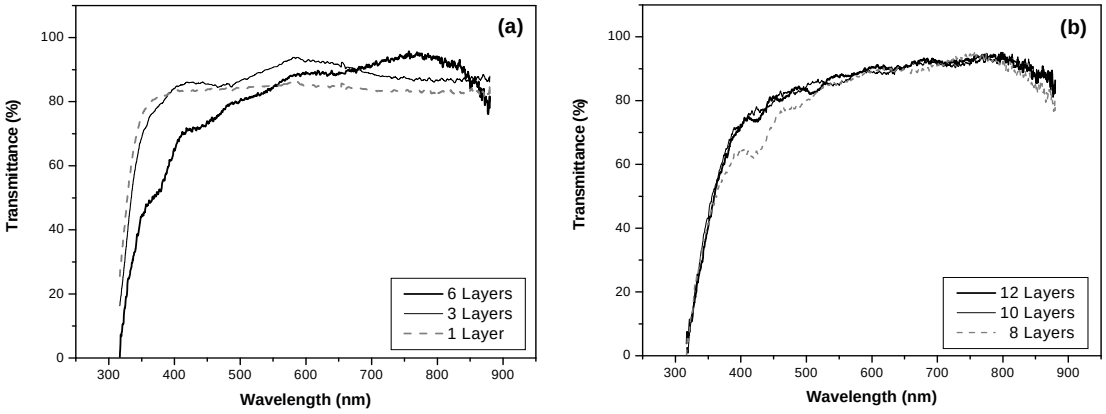


*Fig.6. Optical transmission spectra of multilayered undoped $SnO_2$ films annealed at 673 K.*

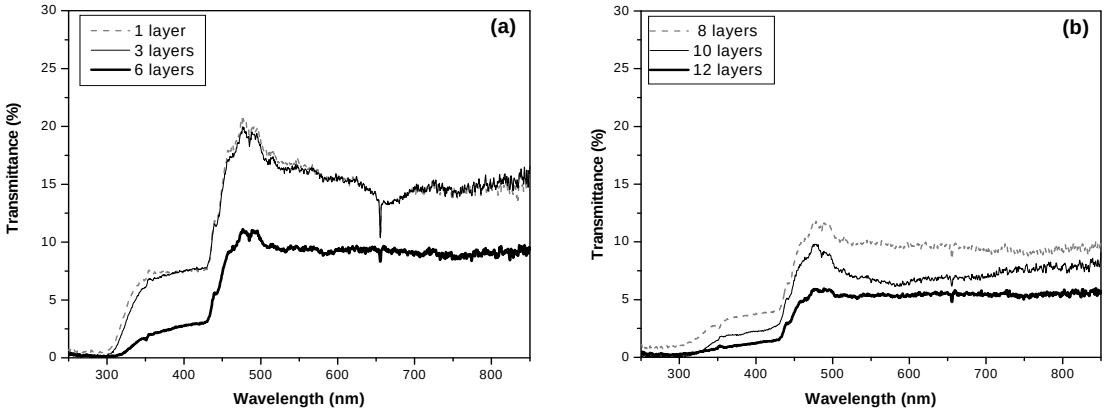


*Fig.7. Optical transmission spectra of multilayered Pd-doped $SnO_2$ films annealed at 673 K.*

The optical analysis report for the palladium doped $SnO_2$ films is shown in fig. 7(a)&(b). With addition of palladium the transparency of the films decreased to a great extent as compared to the undoped $SnO_2$ films. The transmission of the Pd-doped $SnO_2$ films deposited on glass substrates varied from 5% to 20% over the wavelength range 450 to 800 nm. It also shows a clear decrease in the average transmittance values with increase in number of film layers along with fall in transmission at about 310 nm due to the absorption of the glass substrate. The fig 7(a)&(b) shows flat bases on the onset of absorption edges. This may be due to the increase in concentration of $SnO_2$ with Pd-doping as well as formation of bigger crystallites and increased scattering which became remarkable from the SEM images due to the surface roughness.

The band gaps of these films were calculated from fig 6 & fig.7 using the formula [11]:

$$\alpha h\upsilon = A\,(h\upsilon - E_g)^m$$

where $\alpha$ = Absorption coefficient
$h$ = Planck's constant
$\upsilon$ = Frequency of incident light
$E_g$ = Band gap of the material
$m$ = Factor governing the direct/ indirect, etc. transitions of the electrons from the valence band to the conduction band.

It was found that the band gap for undoped $SnO_2$ films varied between 3.61 and 3.86 eV. The band gap decreased considerably for films with increase in number of layers. For representative undoped $SnO_2$ films having one layer, three layers, six layers, eight layers, ten layers and twelve layers the band gaps were found to be 3.86, 3.75, 3.69, 3.66, 3.63 and 3.61 eV

respectively, which are comparable to that of bulk $SnO_2$. The band gap calculated similarly for the Pd-doped $SnO_2$ multilayered films ranges between 3.80 eV and 3.23 eV for one layer and twelve layers respectively. This shows a considerable decrease in the band gap with increase in number of film layers and with doping of $SnO_2$ with palladium.

The deposited $SnO_2$ films' thicknesses were calculated from their optical data using the equation [12]:

$$t = (N_o \lambda_1 \lambda_2) / \{2(n_1 \lambda_2 - n_2 \lambda_1)\} \quad (1)$$

Where, $N_o$= Number of oscillations between two extrema and $n_1$ and $n_2$ represent the refractive indices of the film at wavelengths $\lambda_1$ and $\lambda_2$ respectively. The refractive index was obtained from the relation

$$[(n_a^2+n_g^2)/2 + 2n_a n_g T_o] + [\{(n_a^2+n_g^2)/2 + 2n_a n_g T_o\}^2 - n_a^2 n_g^2]^{1/2} \quad (2)$$

where,

$$T_o = (T_{max} - T_{min}) / T_{max}.T_{min} \quad (3)$$

The films' thicknesses were calculated from the above expressions and were found to vary from 0.18721 to 1.75066 μm for 1-layered and 12-layered undoped $SnO_2$ films respectively. After palladium doping the calculated films' thicknesses ranged between 0.24502 to 1.80054 μm for 1-layered and 12-layered $SnO_2$ films respectively. Film thickness depends upon the preparation techniques (ie. numbers of drops, drop size, rotation speed of the spin coater, etc.) and hence the thicknesses of the films are not always exactly proportional to the number of layers. It has been found to have an error of approximately ±2% after three or four layers of depositions.

### 3.4. I/V characteristics

I/V characteristics for undoped $SnO_2$ is shown in fig. 8(a)& 8(b) and for Pd-doped $SnO_2$ in fig.9 (a)& 9(b) without and with exposure of methane gas respectively. Both the graphs show rising slopes with exposure to the gas. Interestingly the films show a better sensing pattern with increase in the number of film layers. This can be attributed to the decrease in grain boundary and the increase in grain growth with the stacking of film layers along with the cumulative effect of the annealing temperature. It provides a better surface area to interact with the exposed gas. The addition of palladium to the $SnO_2$ films show increase in the conductivity of the $SnO_2$ thin films. These films show even better sensitivity to the methane gas and the changes in their I/V slopes with gas exposure have been depicted in Table-1.

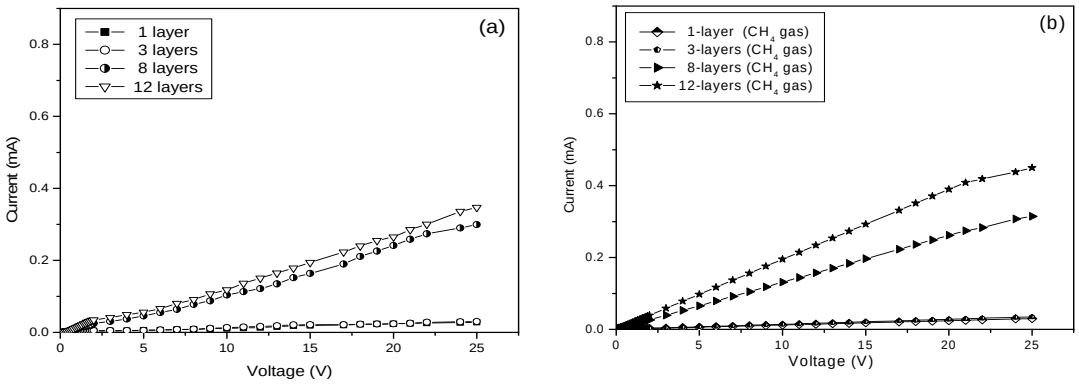


*Fig. 8. I/V curve for undoped $SnO_2$ (a) Without gas exposure (b) With methane gas exposure*

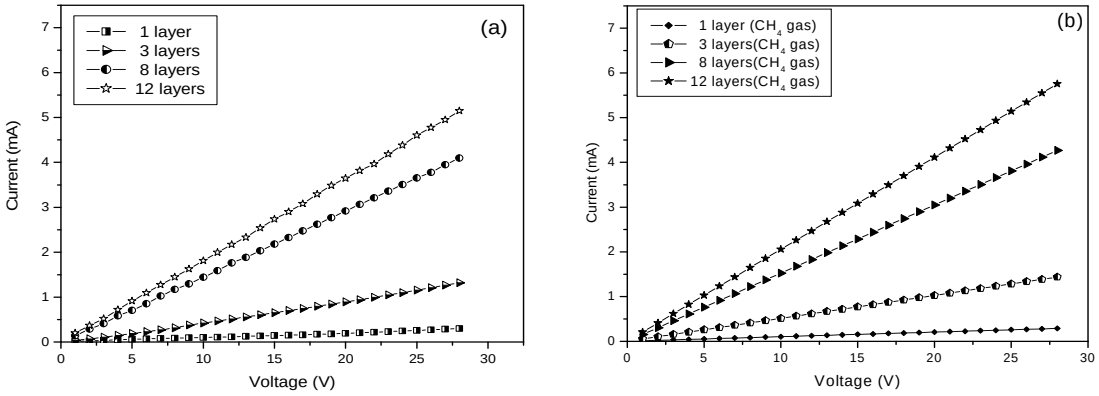


*Fig. 9. I/V curve for Pd-doped $SnO_2$ (a) Without gas exposure (b) With methane gas exposure*

Increase in slopes is a measure of the increase in sensitivity of the films as methane gas sensors. It is observed from table-1 that the sensitivity for doped film is around four times more than that of undoped films for films with eight to twelve layers. Hence multilayer doped $SnO_2$ films can be used as an efficient methane sensor.

Hall measurements (at 2000 G magnetic field) have also been carried out for these films (fig. 10 which support the rising trend in the sensing behavior of these Pd-doped multilayered $SnO_2$ thin films as observed in the I/V characteristics.

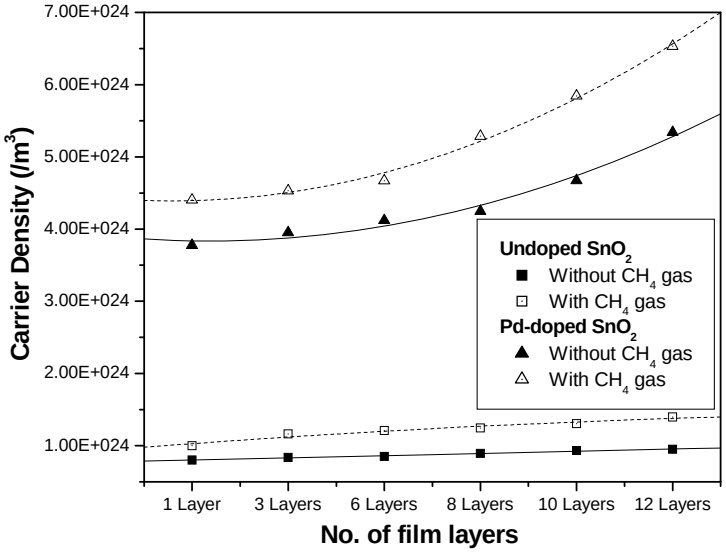


*Fig 10. Variation of carrier densities with no. of layers for undoped and Pd-doped $SnO_2$ thin films.*

Fig. 10 shows increase in carrier concentration with increase in number of film layers for both undoped and Pd-doped $SnO_2$ films when exposed to methane gas. Thus, it shows increase in conductivity, as supported by the increased I/V characteristic slopes and also by the optical data showing gradual decrease in band gap with increased film layers.

### 3.5. Gas sensitivity

The gas sensitivity of undoped and doped $SnO_2$ multi-layered films are calculated from their I/V slopes (fig 8 & 9) with and without methane gas exposure (table-1).

*Table1. Slopes from the I/V curves (after linear fitting) of $SnO_2$ multilayer samples.*

| $SnO_2$ Thin Films Samples | Slope (mA/V) (With exposure to methane gas ) | Slope (mA/V) (Without gas exposure) | Increase in slope (i.e. sensitivity of the samples) |
|---|---|---|---|
| Undoped | | | |
| 1-layer | 0.0012 | 0.0012 | 0 |
| 3-layers | 0.0014 | 0.0013 | 0.0001 |
| 6-layers | 0.0066 | 0.0060 | 0.0006 |
| 8-layers | 0.0131 | 0.0116 | 0.0015 |
| 10-layers | 0.0165 | 0.0124 | 0.0041 |
| 12-layers | 0.0195 | 0.0133 | 0.0062 |
| Pd-Doped | | | |
| 1-layer | 0.0103 | 0.0101 | 0.0002 |
| 3-layers | 0.0180 | 0.0177 | 0.0003 |
| 6-layers | 0.0513 | 0.0497 | 0.0016 |
| 8-layers | 0.1524 | 0.1458 | 0.0066 |
| 10-layers | 0.1887 | 0.1722 | 0.0165 |
| 12-layers | 0.2056 | 0.1825 | 0.0231 |

Generally gas sensitivity(S) calculation is done from the formula $S(\%) = \{(R_{air} - R_{gas})/ R_{air}\}x100$, $R_{air}$ and $R_{gas}$ being the sensor resistance in air and gas at the same temperature[12] which can also be represented in the form $S = (Slope_{gas} - Slope_{air})$ ; $Slope_{air}$ being the slope of the I/V curve in absence of methane and $Slope_{gas}$ being the slope of the I/V curve in presence of methane gas. The difference in the slopes is plotted graphically in fig. 11 to show the sensitivity of the films in presence of 1500 ppm methane gas.

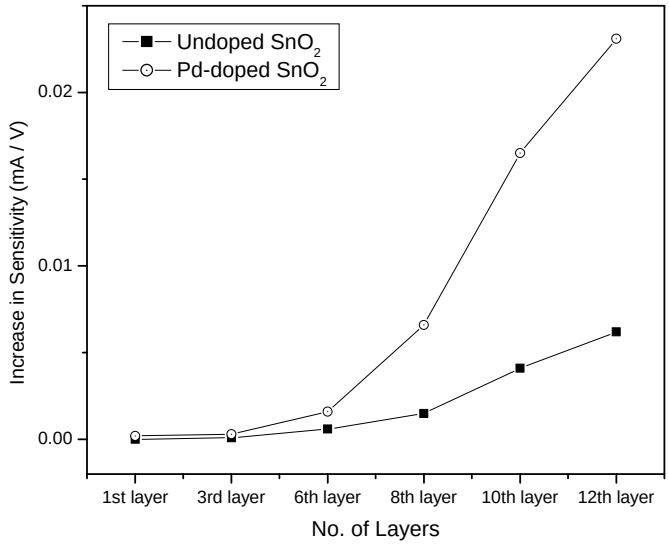


*Fig. 11. Sensitivity of $SnO_2$ to methane gas with increasing number of film layers.*

Due to n-type behavior of $SnO_2$ the electrical conductivity increased with a reducing gas like methane. Experimental results show that tin dioxide is a good methane gas sensor. The resistances of $SnO_2$ films depend on the various oxygen deficient sites present after deposition as well as on the doping level. With little incorporation of palladium onto $SnO_2$, it resides on the grains and at the grain boundaries of the films. Palladium doped over the $SnO_2$ films generate

surface states and provides excess electrons to them. The gas response is further enhanced by the buildup of film layers and is evident from the optical data which shows decrease in the calculated band gaps with increase in the film layers showing better conductivity.

## 4. Conclusions

In this work we have deposited and characterized sol-gel prepared multilayered undoped and Pd-doped $SnO_2$ thin films. Electrical and hall measurements were carried out and it has been found that undoped $SnO_2$ is a mild methane gas sensor at room temperature. However its sensitivity can be increased with the addition of a catalyzing agent like palladium and can further be improved by the build up of multiple layers. The above result may be utilized to design an efficient methane gas sensor for environmental health and safety.

## References

[1] K. Anothainart, M. Burgmair, A. Karthigeyan, M. Zimmer, I. Eisele, Sensors and Actuators B: Chemical **93**, 580 (2003).
[2] Z. A. Ansari, S. G. Ansari, T. Ko, J.-H. Oh, Sensors and Actuators B:Chemical **87**, 105 (2002).
[3] A. Cabot, J. Arbiol, J.R. Morante, U. Weimar, N. Barsan, W. Gopel, Sensors and Actuators B: Chemical **70**, 87 (2000).
[4] A. Chiorino, G. Ghiotti, F. Prinetto, M.C. Carotta, D. Gnani, G. Martinelli, Sensors and Actuators B: Chemical **58**, 338 (1999).
[5] G. G. Mandayo, E. Castano, F.J. Gracia, A. Cirera, A., Cornet, J.R. Morante, Sensors and Actuators B: Chemical **95**, 90 (2003).
[6] R.S. Niranjan, K.R. Patil, S.R. Sainkar and I.S. Mulla, Mater. Chem. Phys. **80**, 250 (2003).
[7] L. Jianping, W. Yue, G. Xiaoguang, M. Qing, W. Li and H. Jinghong, Sensors and Actuators B: Chemical **65**, 111 (2000).
[8] Mc Carthy, G., Welton, J., Powder Diffraction, **4**, 156 (1989)
[9] Y.-S. Lee, O.-S. Kwon, S.-M. Lee, K.-D. Song, C.-H. Shim, G.-H. Rue, D.-D. Lee, Sensors and Actuators B: Chemical **93**, 556 (2003).
[10] S.A. Mahmoud, A.A. Akl, H. Kamal, K. Abdel-Hady, Physical B **311**, 336 (2002).
[11] S. Majumder, S. Hussain, R. Bhar, A.K. Pal, Vacuum **81**, 985 (2007).
[12] A. Sarkar, S. Ghosh, S. Chaudhuri, A.K. Pal, Thin Solid Films **204**, 255 (1991).